

Finite-size effects on the chiral phase diagram of four-fermion models in four dimensions

L.M. Abreu^{a,*} A.P.C. Malbouisson^b J.M.C. Malbouisson^c,
A.E. Santana^d

^a*Centro de Ciências Exatas e Tecnológicas, Universidade Federal do Recôncavo da Bahia, 44380-000, Cruz das Almas, BA, Brazil*

^b*Centro Brasileiro de Pesquisas Físicas/MCT, 22290-180, Rio de Janeiro, RJ, Brazil*

^c*Instituto de Física, Universidade Federal da Bahia, 40210-340, Salvador, BA, Brazil*

^d*Instituto de Física, Universidade de Brasília, 70910-900, Brasília, DF, Brazil*

Abstract

We study the size dependence of the dynamical symmetry breaking in the four-dimensional Nambu-Jona-Lasinio model. We show that the presence of boundaries reduces the chiral breaking region, and this effect is strengthened for a larger number of compactified dimensions. A critical value for the length of the compactified dimensions exists, below which the dynamical symmetry breaking is not possible. Considering finite temperature and chemical potential, the chiral phase structure for the system with compactified dimensions is obtained. A gradual decreasing of the chiral breaking region with increasing of chemical potential is found. Also, at fixed chemical potential, the decreasing of the size of the system changes the order of the chiral phase transition.

Key words: Four-fermion models, dynamical symmetry breaking, finite-size effects

PACS: 11.30.Rd, 12.40.-y, 12.39.Fe, 11.10.Wx

* Corresponding author

Email addresses: lmabreu@ufrb.edu.br (L.M. Abreu), adolfo@cbpf.br (A.P.C. Malbouisson), jmalboui@ufba.br (J.M.C. Malbouisson), asantana@fis.unb.br (A.E. Santana).

1 Introduction

The phase structure of the strongly interacting matter attracts a great deal of interest. Due to the intricate mathematical structure of Quantum Chromodynamics (QCD), effective models that incorporate some of its properties have been largely employed. In this sense, four-fermion models, as the Nambu-Jona-Lasinio (NJL) model [1], are very useful for the investigation of dynamical symmetries when the system is under certain conditions, like finite temperature, finite chemical potential, gravitational field, etc. [2,3,4]. In particular, an interesting aspect in the analysis of the phase transitions of four-fermion models is the effect of space compactification [5,6,7,8,9,10,11,12]. Boundary effects have also been considered for quark-meson models [13,14]. The general question is to estimate the relevance of the fluctuations due to finite-size effects in the phase diagram. With this purpose, different approaches have been used to study various aspects of these models, as the finite-size scaling analysis [7], the multiple reflection expansion [10], and the zeta-function method [11].

In this paper, we extend the techniques introduced in Ref. [11] and investigate finite-size effects on the dynamical symmetry breaking of the four-dimensional NJL model at finite temperature and chemical potential. This is done in the framework of zeta-function regularization and compactification methods [15]. This approach allows in a simple way to determine analytically the size-dependence of the effective potential and the gap equation. Then, phase diagrams at finite temperature and chemical potential, where the symmetric and broken phases are separated by size-dependent critical lines, are obtained. Note that our approach leads to exact results within the mean-field (Hartree) theory without making use of any additional approximation. This allows to avoid, for example, difficulties appearing in calculating the density of states using the multiple reflection expansion, as pointed out in Ref. [16].

We organize the paper as follows. In Section II, we calculate the effective potential of the NJL model in the mean-field approximation, using the zeta-function method. The size-dependent gap equation is discussed in Section III, while the phase diagrams are shown and analyzed in Section IV. Finally, Section V presents some concluding remarks.

2 The formalism

Our starting point is the massless version of the NJL model, described by the Lagrangian density,

$$\mathcal{L} = \bar{q}i\not{\partial}q + \frac{G}{2} \sum_{a=0}^{N^2-1} [(\bar{q}\alpha^a q)^2 + (\bar{q}i\gamma_5\alpha^a q)^2], \quad (1)$$

where q and \bar{q} are the N -component spinors, and the matrices α^a are the generators of the group $U(N)$, with $\alpha^0 = \mathbf{I}/\sqrt{N}$.

We perform the bosonization assuming that only one auxiliary field, that associated with the bilinear $\bar{q}\alpha^0 q$, takes non-vanishing values. This auxiliary field, denoted here by σ , plays the role of a dynamical fermion mass, such that when it has a non-vanishing value, the system is in the chiral broken phase. We shall work in the Euclidian space, performing the Wick rotation in the time coordinate. For generality, we consider the D -dimensional Euclidean space-time, restricting latter to the $D = 4$ case. Besides, taking σ uniform, i.e. independent of coordinates, we obtain the effective potential up to one-loop order, at leading order in $\frac{1}{N}$, as

$$\frac{1}{N}U_{eff} = \frac{\mathcal{A}_{eff}}{V} = \frac{\sigma^2}{2G} + U_1(\sigma), \quad (2)$$

where \mathcal{A}_{eff} is the effective action, V is the volume and

$$U_1(\sigma) = -h_D \int \frac{d^D k}{(2\pi)^D} \ln \left(\frac{k_E^2 + \sigma^2}{\lambda^2} \right). \quad (3)$$

Above, h_D is the dimension of the Dirac representation and λ is a scale parameter.

To take into account finite-size effects on the phase structure of this model, the system is considered to have d ($\leq D$) compactified dimensions. We denote the Euclidian coordinate vectors by x_E and write $x_E = (y, z)$, where

$$y = (y_1 \equiv x_E^1, \dots, y_n \equiv x_E^n), \quad z = (z_1 \equiv x_E^{n+1}, \dots, z_d \equiv x_E^D), \quad (4)$$

with the z_j component being defined in the interval $[0, L_j]$ and $n = D - d$, corresponding to the topology $\mathbb{R}^n \times \mathbb{S}^{1_{n+1}} \times \dots \times \mathbb{S}^{1_d}$ where \mathbb{S}^{1_j} is a circumference of radius L_j . Therefore, the compactification of the z -coordinates makes the k_z -components of the momentum k_E to assume discrete values,

$$k_z^j \rightarrow \frac{2\pi}{L_j}(n_j + c_j), \quad (5)$$

where $n_j = 0, 1, 2, \dots$ and $c_j = \frac{1}{2}$ ($j = 1, 2, \dots, d$) for antiperiodic boundary conditions. Note that we may associate a given L_j with the inverse of temperature $\beta = 1/T$, say $L_{j_0} \equiv \beta$, thus treating the system at finite temperature with $d-1$ compactified spatial dimensions. In this case, a finite chemical potential, μ , can also be introduced through the rule $c_{j_0} = \frac{1}{2} - \frac{i\beta\mu}{2\pi}$.

In the following, we use the zeta-function regularization method [15], rewriting Eq. (3) as

$$U_1(\sigma) = \frac{h_D}{2V} \left[\zeta'(0) + \ln \lambda^2 \zeta(0) \right], \quad (6)$$

where $\zeta(s)$ is given by

$$\zeta(s) = V_n \sum_{n_1, \dots, n_d = -\infty}^{+\infty} \int \frac{d^n k_y}{(2\pi)^n} \left[k_z^2 + k_y^2 + \sigma^2 \right]^{-s}, \quad (7)$$

where $k_z^2 = \sum_{j=1}^d \frac{4\pi^2}{L_j^2} (n_j + c_j)^2$, with V_n being the n -dimensional volume. The techniques of dimensional regularization can be used to perform the integration over the non-compactified k_y -components, yielding

$$\zeta(s; \{a_j\}, \{c_j\}) = \frac{V_n}{(4\pi)^{n/2}} \frac{\Gamma\left(s - \frac{n}{2}\right)}{\Gamma(s)} Y_d^{\sigma^2} \left(s - \frac{n}{2}; \{a_j\}, \{c_j\} \right), \quad (8)$$

where $Y_d^{\sigma^2}(\nu; \{a_j\}, \{c_j\})$ is the generalized Epstein-zeta function, defined by

$$Y_d^{\sigma^2}(\nu; \{a_j\}, \{c_j\}) = \sum_{n_1, \dots, n_d = -\infty}^{+\infty} \left[a_1 (n_1 + c_1)^2 + \dots + a_d (n_d + c_d)^2 + \sigma^2 \right]^{-\nu}, \quad (9)$$

with $a_j = 4\pi^2/L_j^2$. Note that $Y_d^{\sigma^2}$ is well-defined only for $\text{Re } \nu > d/2$, but it can be analytically continued, becoming a meromorphic function, into the whole complex ν -plane.

As remarked in Refs. [15,11], the analysis of the pole structure of the zeta-function implies that Eq. (6) must be written as

$$U_1(\sigma; \{a_j\}, \{c_j\}) = \frac{h_D}{2V_d(4\pi)^{n/2}} \Gamma\left(-\frac{n}{2}\right) Y_d^{\sigma^2} \left(-\frac{n}{2}; \{a_j\}, \{c_j\}\right), \quad (10)$$

for n odd, or

$$U_1(\sigma; \{a_j\}, \{c_j\}) = \frac{h_D}{2V_d(4\pi)^{n/2}} \frac{(-1)^{\frac{n}{2}}}{\frac{n}{2}!} \left\{ Y_d^{\sigma^2 \prime} \left(-\frac{n}{2}; \{a_j\}, \{c_j\}\right) + Y_d^{\sigma^2} \left(-\frac{n}{2}; \{a_j\}, \{c_j\}\right) \left[\ln \lambda^2 - \gamma - \psi \left(\frac{n}{2} + 1\right) \right] \right\}, \quad (11)$$

for n even, where γ and $\psi(s)$ denote the Euler-Mascheroni constant (≈ 0.5772) and the digamma function, respectively. Both expressions will be used in the

discussion of symmetry breaking in the four-dimensional NJL model with compactified dimensions.

3 The gap equation

The phase structure of the model is studied through the gap equation, obtained by minimizing the effective potential with respect to σ ,

$$\left. \frac{\partial}{\partial \sigma} U_{eff}(\sigma; \{a_j\}, \{c_j\}) \right|_{\sigma=m} = 0, \quad (12)$$

where m is the order parameter of the chiral phase transition, that is the dynamically generated fermion mass. We now discuss the size effects on the gap equation starting, for completeness and to set the free space parameters, by treating the model in absence of boundaries.

3.1 Non-compactified model

Let us consider the NJL model in four dimensions without compactified dimensions. This corresponds to $d = 0$, and so $n = D = 4$. This system has been treated in the literature (see Refs. [17,18] for reviews) using other methods. With the zeta-function approach, the renormalized effective potential is given by

$$\frac{1}{N} U_{eff}(\sigma; d=0) = \frac{\sigma^2}{2G_R} + \frac{h_D(D-1)}{(4\pi)^{D/2}} \Gamma\left(1 - \frac{D}{2}\right) \lambda^{D-2} \sigma^2 - \frac{h_D}{D(4\pi)^{D/2}} \Gamma\left(1 - \frac{D}{2}\right) \sigma^D, \quad (13)$$

where the renormalized coupling constant G_R is defined by

$$\frac{1}{G_R} = \frac{1}{G} - \frac{h_D(D-1)}{(4\pi)^{D/2}} \Gamma\left(1 - \frac{D}{2}\right) \lambda^{D-2}. \quad (14)$$

Note that Eq. (13) is valid for $2 \leq D < 4$; it is singular for $D = 4$, due to the pole of the gamma-function. In the limit $D \rightarrow 4$, we define $\epsilon = 4 - D$ and obtain an analytically regularized effective potential, taking $h_D = 4$, as

$$\begin{aligned} \frac{1}{N} \frac{U_{eff}(\sigma)}{\lambda^4} &= \frac{1}{2G_R} \frac{\sigma^2}{\lambda^4} - \frac{6\sigma^2}{(4\pi)^2 \lambda^2} \left(\frac{1}{\epsilon} - \gamma + \ln 4\pi + \frac{1}{3} \right) \\ &+ \frac{\sigma^4}{(4\pi)^2 \lambda^4} \left(\frac{1}{\epsilon} - \gamma + \ln 4\pi + \frac{3}{2} - \ln \frac{\sigma^2}{\lambda^2} \right); \end{aligned} \quad (15)$$

this shows explicitly the singular behavior of Eq. (13) as $\epsilon \rightarrow 0$.

Let us compare Eq. (15) with the corresponding expression obtained by using the cut-off regularization [17,18],

$$\frac{1}{N} \frac{U_{eff}(\sigma)}{\lambda^4} = \frac{1}{2G} \frac{\sigma^2}{\lambda^4} - \frac{6\sigma^2}{(4\pi)^2 \lambda^2} \left(\ln \frac{\Lambda^2}{\lambda^2} - \frac{2}{3} \right) + \frac{\sigma^4}{(4\pi)^2 \lambda^4} \left(\ln \frac{\Lambda^2}{\lambda^2} + \frac{1}{2} - \ln \frac{\sigma^2}{\lambda^2} \right), \quad (16)$$

where Λ is the cut-off parameter which must be larger than λ . Thus, the zeta-function and cut-off methods are equivalent through the correspondence

$$\frac{1}{\epsilon} - \gamma + \ln 4\pi + 1 \leftrightarrow \ln \frac{\Lambda^2}{\lambda^2}. \quad (17)$$

Hence, with the use of the correspondence in Eq. (17), the non-trivial solution of the gap equation derived from Eq. (15) can be written as

$$\frac{1}{G_c} - \frac{1}{G_0} = -\frac{1}{m\lambda^2} \left. \frac{\partial}{\partial \sigma} U_1(\sigma) \right|_{\sigma=m} = \frac{4m^2}{(4\pi)^2 \lambda^2} \ln \frac{\Lambda^2}{m^2}, \quad (18)$$

where we have defined the dimensionless coupling constant $G_c = \lambda^2 G_R$, and

$$\frac{1}{G_0} = \left. \frac{\partial}{\partial \sigma} U_{eff}(\sigma) \right|_{\sigma \rightarrow 0} = \frac{12}{(4\pi)^2} \left(\ln \frac{\Lambda^2}{\lambda^2} - \frac{2}{3} \right). \quad (19)$$

In Eq. (18), it is possible to identify the constant G_0 acting as a critical value; when $G_c > G_0$ we have dynamically generated fermion mass. A value for G_0 can be fixed by choosing values for the mass scale λ and the cut-off Λ from phenomenological arguments; note that, for $D = 4$, the NJL model has to be considered as an effective model.

3.2 Presence of boundaries

To take into account temperature and finite-size effects, we must analyze the modified gap equation,

$$\frac{1}{G_c} - \frac{1}{G_0} = -\frac{1}{\bar{m}\lambda^2} \left. \frac{\partial}{\partial \sigma} U_1(\sigma; \{a_j\}, \{c_j\}) \right|_{\sigma=\bar{m}}, \quad (20)$$

where $\bar{m} = \bar{m}(\{a_j\}, \{c_j\})$ is the boundary modified fermion mass. Then, accordingly to the zeta-function approach, using Eqs. (10) and (11), the modified gap equation, Eq. (20), is written as

$$\frac{1}{G_c} = \frac{1}{G_0} + \frac{4}{\lambda^2 V_d (4\pi)^{n/2}} \Gamma\left(1 - \frac{n}{2}\right) Y_d^{\bar{m}^2} \left(-\frac{n}{2} + 1; \{a_j\}, \{c_j\}\right), \quad \text{for } d = 1, 3; \quad (21)$$

while it has the form

$$\begin{aligned} \frac{1}{G_c} &= \frac{1}{G_0} + \frac{4}{\lambda^2 V_2 4\pi} \left\{ Y_2^{\overline{m}^2}{}' (0; \{a_j\}, \{c_j\}) \right. \\ &\quad \left. + Y_2^{\overline{m}^2} (0; \{a_j\}, \{c_j\}) \left[\ln \lambda^2 - \gamma - \psi(1) \right] \right\}, \quad \text{for } d = 2; \end{aligned} \quad (22)$$

and finally,

$$\frac{1}{G_c} = \frac{1}{G_0} - \frac{4}{\lambda^2 V_4} \text{FP} \left[Y_4^{\overline{m}^2} (1; \{a_j\}, \{c_j\}) \right], \quad \text{for } d = 4, \quad (23)$$

where $\text{FP}[Y_4^{\overline{m}^2}]$ means the finite part of $Y_4^{\overline{m}^2}$.

Thus, taking the fermion mass approaching to zero in Eqs. (21), (22) and (23), we obtain the critical values of the coupling constant G_c with the corrections due to the presence of boundaries, for the cases $d = 1, 3$, $d = 2$ and $d = 4$, respectively. In this context, $Y_d^{\overline{m}^2} \Big|_{\overline{m}^2 \rightarrow 0}$ reduces to a homogeneous generalized Epstein zeta-function Y_d .

The next step is the construction of analytical continuations for Y_d , which are written through a generalized recurrence formula [11],

$$\begin{aligned} Y_d(\nu; \{a_j\}, \{c_j\}) &= \frac{\Gamma\left(\nu - \frac{1}{2}\right)}{\Gamma(\nu)} \sqrt{\frac{\pi}{a_d}} Y_{d-1}\left(\nu - \frac{1}{2}; \{a_{j \neq d}\}, \{c_{j \neq d}\}\right) \\ &\quad + \frac{4\pi^s}{\Gamma(\nu)} W_d\left(\nu - \frac{1}{2}; \{a_j\}, \{c_j\}\right), \end{aligned} \quad (24)$$

where the symbol $\{a_{j \neq d}\}$ means that the parameter a_d is excluded from the set $\{a_j\}$, and

$$W_d(\eta; \{a_j\}, \{c_j\}) = \frac{1}{\sqrt{a_d}} \sum_{\{n_j \neq d \in \mathbb{Z}\}} \sum_{n_d=1}^{\infty} \cos(2\pi n_d c_d) \left(\frac{n_d}{\sqrt{a_d} X_{d-1}} \right)^\eta K_\eta \left(\frac{2\pi n_d}{\sqrt{a_d}} X_{d-1} \right); \quad (25)$$

in the above equation $X_{d-1} = \sqrt{\sum_{k=1}^{d-1} a_k (n_k + c_k)^2}$ and $K_\nu(z)$ is the modified Bessel function of second kind (see Refs. [19,20] for a discussion of the $a_j \leftrightarrow a_l$ symmetry).

4 Phase structure

4.1 Finite-size effects on the critical coupling

We now analyze the L_j -dependent critical curves for the phase diagram from the gap equation in the limit $\overline{m} \rightarrow 0$. First, we study the compactification

of spatial coordinates at zero temperature. Thus, we take Eq. (21) in the cases $d = 1$ and $d = 3$, and Eq. (22) for the $d = 2$ case. After that, we use the recurrence formula, given by Eq. (24), and perform the necessary manipulations.

Considering the simplest situation in which all spatial coordinates are restricted to intervals of the same length and obey antiperiodic boundary conditions, i.e. $L_j = L$ and $c_j = 1/2$ for $j = 1, \dots, d$, we obtain the following gap equations

$$\frac{1}{G_c} = \frac{1}{G_0} - \frac{A_d}{(L\lambda)^2}, \quad (26)$$

where

$$A_1 = \frac{1}{6} \approx 0.16, \quad (27)$$

$$A_2 = A_1 - \frac{4}{\pi} \sum_{n_1=-\infty}^{\infty} \sum_{n_2=1}^{\infty} (-1)^{n_2} \left(\frac{|n_1 + \frac{1}{2}|}{n_2} \right)^{\frac{1}{2}} K_{-\frac{1}{2}} \left(2\pi n_2 \left| n_1 + \frac{1}{2} \right| \right) \approx 0.22, \quad (28)$$

$$A_3 = A_2 - \frac{4}{\pi} \sum_{n_1, n_2=-\infty}^{\infty} \sum_{n_3=1}^{\infty} (-1)^{n_3} K_0 \left(2\pi n_3 \sqrt{\sum_{i=1}^2 \left(n_i + \frac{1}{2} \right)^2} \right) \approx 0.26. \quad (29)$$

To illustrate the results above, in Fig. 4.1 we plot the critical coupling constant G_c , given by Eq. (26), as a function of $x = (L\lambda)^{-1}$, with the coefficient A_d taking the values given by Eqs. (27), (28) and (29); we also fix the value of $G_0 \simeq 5.66$, obtained from Eq. (19) by choosing $\Lambda \approx 1.25$ GeV and $\lambda \approx 280$ MeV [21]. The three cases considered correspond, respectively, to the system between two parallel planes a distance L apart; in the form of an infinite cylinder having a square transverse section of area L^2 ; in the form of a cubic box of volume L^3 . For each situation the chiral breaking region corresponds to the region above the corresponding line. Since G_c increases as L decreases, we can infer that the finite-size effects require a stronger interaction to maintain the system in the chiral breaking region, as L is diminished.

We also find from Eq. (26) that, for each d , a critical value L_c exists below which the chiral breaking region is completely suppressed; this critical value is obtained by setting the right hand side of Eq. (26) equal to zero. For $G_0 \simeq 5.66$, considering the values of A_d given by Eqs. (27–29), we get $x_c = (L_c\lambda)^{-1} \simeq 1.03$ for $d = 1$, $x_c \simeq 0.89$ for $d = 2$ and $x_c \simeq 0.83$ for $d = 3$. We see that the cubic box has the greatest value of L_c , which means that the largest number of compactified dimensions is the scenario which needs the strongest interaction to keep the system in the chiral breaking region.

It is worth noting that the behavior of the critical coupling constant as a

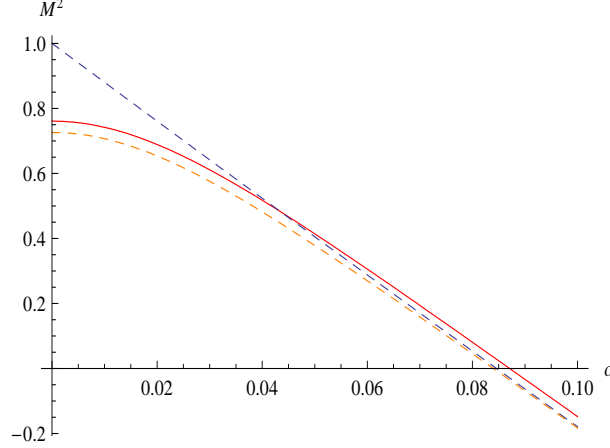


Fig. 1. The critical coupling constant G_c , Eq. (26), as a function of $x = (L\lambda)^{-1}$. The dashed, dotted and solid lines correspond to the cases of $d = 1, 2, 3$ compactified dimensions, respectively, with A_d given by Eqs. (27–29). We fixed $G_0 \simeq 5.66$.

function of L does not depend on the number of compactified dimensions, as it is expected from finite-size scaling arguments.

4.2 System at finite temperature

Now we consider the system with compactified spatial dimensions and at finite-temperature. Since the way of introducing finite-size effects is through a generalized Matsubara prescription, we can identify one of the compactified dimensions with the Euclidian (imaginary) time and take the compactification length as the inverse of the temperature, say $L_1 = \beta \equiv T^{-1}$. So, to analyze the (L, T) -dependent phase diagram, we must look at the critical equation obtained from Eqs. (18) and (20),

$$\frac{4m^2}{(4\pi)^2\lambda^2} \ln \frac{\Lambda^2}{m^2} + \frac{1}{\bar{m}\lambda^2} \frac{\partial}{\partial\sigma} U_1(\sigma; \{a_j\}, \{c_j\}) \Big|_{\sigma=\bar{m}} = 0, \quad (30)$$

where $a_1 = 4\pi^2/L_1^2 \equiv 4\pi^2/\beta^2$ and, for simplicity, we take $a_2 = \dots = a_d = 4\pi^2/L^2$. Then, we look at Eq. (22) for $d = 2$, Eq. (21) for $d = 3$, and Eq. (23) for $d = 4$ considering, in all these cases, $L_1 = \beta$. Next, we perform the necessary manipulations, in an analogous way as we have done in the previous subsection, and take the limit $\bar{m} \rightarrow 0$. Thus, using Eqs. (24) and (25), we obtain

$$\frac{4m^2}{(4\pi)^2} \ln \frac{\Lambda^2}{m^2} - \frac{A_1}{L^2} + \frac{4}{\pi L} \sum_{n_1=-\infty}^{\infty} \sum_{n_2=1}^{\infty} (-1)^{n_2} \left(\frac{|n_1 + \frac{1}{2}|}{n_2\beta L} \right)^{\frac{1}{2}} K_{-\frac{1}{2}} \left(2\pi n_2 \frac{\beta}{L} \left| n_1 + \frac{1}{2} \right| \right) = 0, \quad (31)$$

for $d = 2$;

$$\begin{aligned}
& \frac{4m^2}{(4\pi)^2} \ln \frac{\Lambda^2}{m^2} - \frac{A_2}{L^2} \\
& + \frac{4}{\pi L^2} \sum_{n_1, n_2 = -\infty}^{\infty} \sum_{n_3 = 1}^{\infty} (-1)^{n_3} K_0 \left(2\pi n_3 \frac{\beta}{L} \sqrt{\left(n_1 + \frac{1}{2}\right)^2 + \left(n_2 + \frac{1}{2}\right)^2} \right) = 0,
\end{aligned} \tag{32}$$

for $d = 3$; and finally

$$\begin{aligned}
& \frac{4m^2}{(4\pi)^2} \ln \frac{\Lambda^2}{m^2} - \frac{A_3}{L^2} + \frac{4}{\pi L^3} \sum_{n_1, n_2, n_3 = -\infty}^{\infty} \sum_{n_4 = 1}^{\infty} (-1)^{n_4} \left(\frac{n_4 \beta L}{\sqrt{\sum_{i=1}^3 \left(n_i + \frac{1}{2}\right)^2}} \right)^{\frac{1}{2}} \\
& \times K_{\frac{1}{2}} \left(2\pi n_4 \frac{\beta}{L} \sqrt{\sum_{i=1}^3 \left(n_i + \frac{1}{2}\right)^2} \right) = 0,
\end{aligned} \tag{33}$$

in the case of $d = 4$, where A_d , for $d = 1, 2, 3$, are given by Eqs. (27)–(29).

In Fig. ??, we plot the phase diagrams corresponding to Eqs. (31–33) in the (x, T) -plane, where x and T are the inverse of the compactification length and the temperature, respectively, measured in units of m , that is $x = (Lm)^{-1}$ and $T = (\beta m)^{-1}$. Each critical line separates the chiral breaking region, below the line, from the chiral restoration phase, above the line.

In the limit $x \rightarrow 0$, corresponding to the system without spatial boundaries, the critical temperature is $T_c \approx 0.68 m$. The size effects start to appear for $x \approx 0.3$. We see from the curves that the critical temperature decreases as the size of the system diminishes. Our results indicates that there is a minimal size of the system for the existence of a chiral broken phase. The critical values of the compactification lengths for suppression of the chiral breaking region are given by: $x_c = (L_c m)^{-1} = 0.68$ for $d = 2$, $x_c = 0.58$ for $d = 3$ and $x_c = 0.54$ for $d = 4$. Note that, for the system between two parallel planes a distance L apart (the case $d = 2$), the critical line is symmetric by the change $x \leftrightarrow T$, as expected. It can also be seen that the critical temperature has a faster decreasing with the size reduction for the system in the form of a cubic box. This fact is confirmed by the greatest value of the critical length (the length for which the critical temperature vanishes) in this case.

In order to obtain a quantitative estimate for our results, we consider m as the constituent quark mass, $m = 280$ GeV according to Ref. [21]. In this scenario, with the appropriate conversions, the critical temperature for the system without spatial boundaries is $T_c \simeq 0.68 m \approx 190$ MeV and the size effects begin to be noted for $L = (xm)^{-1} \approx 2.4$ fm. For this choice of m , the critical values of the compactification length are $L_c = (x_c m)^{-1} \approx 1.1$ fm for $d = 2$, $L_c = 1.23$ fm for $d = 3$ and $L_c = 1.32$ fm for $d = 4$.

4.3 System at finite temperature and at finite chemical potential

The phase diagram can also be studied by taking into account the dependence on the chemical potential. As previously remarked, this is done by taking in the prescription (5), for the momentum associated with the compactified Euclidian time, $L_1 \equiv \beta = 1/T$ and $c_1 = \frac{1}{2} - \frac{i\beta\mu}{2\pi}$. Thus, considering the simplest situation, $d = 1$, which corresponds to the system in bulk (absence of boundaries), the use of Eqs. (18) and (21) leads to the following equation for the critical line,

$$\frac{4m^2}{(4\pi)^2} \ln \frac{\Lambda^2}{m^2} - \frac{1}{6\beta^2} - \frac{\mu^2}{2\pi^2} = 0. \quad (34)$$

Now, if we consider the system with compactified spatial coordinates, the μ -dependence appears as additional factors in the last term of the left hand side of Eqs. (31), (32) and (33), which are obtained after the appropriate analytical continuation.

So far we have considered only second-order phase transitions. However, the inclusion of a finite chemical potential can alter the nature of the chiral phase transition. To understand as this happens we proceed as follows. We expand the gap equation (20) for \overline{m} near criticality, obtaining

$$A(T, L_j, \mu) + B(T, L_j, \mu)\overline{m}^2 + C(T, L_j, \mu)\overline{m}^4 = 0, \quad (35)$$

where the coefficients $A(T, L_j, \mu)$, $B(T, L_j, \mu)$ and $C(T, L_j, \mu)$ are defined according to Eqs. (21)–(23), i.e. in terms of homogeneous generalized Epstein zeta-functions $Y_d(\nu)$, with different ν -exponents. The tricritical point is then determined by imposing the condition

$$B(T, L_j, \mu) = 0. \quad (36)$$

As an example, in Fig. 4.3 we plot the phase diagram in the (μ, T) -plane for the case without boundaries ($d = 1$). We identify the solid and dashed lines as representing, respectively, second- and first-order phase-transition lines. The dot locates the tricritical point, which occurs at $T_c \simeq 0.46 m \approx 128$ MeV and $\mu_c \simeq 0.90 m \approx 252$ MeV. As expected, at high temperature or low chemical potential, a second-order phase transition is suggested, while in the low-temperature or high-chemical potential limit the system experiments a first-order transition.

Finally, in Fig. ?? we plot the phase diagram of the system with three compactified spatial dimensions ($d = 4$) in the (x, T) -plane, for some values of the chemical potential. The chiral breaking region is gradually diminished with increasing chemical potential. So, when μ increases, lower values of temperature and smaller sizes are necessary to reach a phase-transition line. In addition,

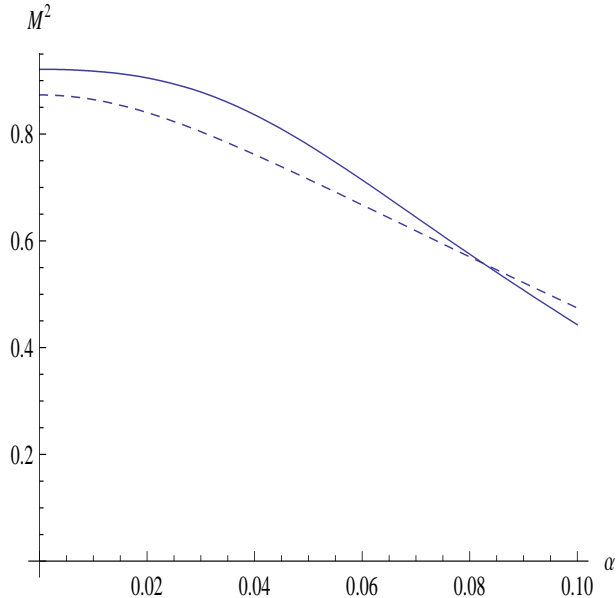


Fig. 2. The phase diagram in the (μ, T) -plane for the case without boundaries ($d = 1$), with T and μ measured in units of m . Solid and dashed lines represent the second-order and first-order phase transition lines, respectively, and the dot is the tricritical point. The chiral breaking region is below the line. Here we take $\frac{\Lambda}{m} = 4.46$ [21].

nonzero values of the chemical potential can alter the order of the phase transition, as expected. Nevertheless, the decreasing of the size can also changes the order of the phase transition for the system at fixed μ .

5 Concluding Remarks

In this work, we have studied dynamical symmetries of a four-fermion model when the system is under certain conditions. We have investigated finite-size effects on the chiral phase structure of the four dimensional NJL model employing zeta-function regularization and compactification methods. In the mean field approximation, this allows to derive analytically expressions of the gap equation when d (≤ 4) dimensions are compactified.

First, the dependence of the critical coupling constant on the size of the system was analyzed, comparing the cases of one, two and three compactified spatial dimensions with the same compactification length L . The presence of boundaries implies that a stronger interaction is needed to maintain the system in the chiral broken phase; this effect is stronger for greater number of compactified dimensions. It is shown that there is a minimal size of the system below which there is no chiral breaking region; the corresponding critical values of the compactification lengths, for $d = 1, 2, 3$, are determined.

The chiral phase structure at finite temperature was investigated by taking one of the compactification lengths, that associated with the compactified Euclidian time, equal to the inverse of temperature. The results suggest that, as the size of the system diminished, finite-size effects start to appear for a given value of the compactification length, with the temperature rapidly decreasing as $1/L$ is further increased; this behavior is more accentuated for the case with the greater number of compactified spatial dimensions, giving the largest decreasing of the chiral breaking region.

The study is concluded with the analysis of the dependence of the chiral phase transition on the chemical potential. For the bulk system, i.e. the system without spatial boundaries, we get a simple expression for the phase-transition line, showing that the critical temperature decreases as the chemical potential increases. The nature of the phase transition changes from second- to first-order at specific values of μ and T which locates the tricritical point. For the system with compactified spatial dimensions, we find that the chiral breaking region decreases as the chemical potential is increased; that is, when μ increases, lower values of temperature and smaller sizes are necessary to keep the system in chiral broken phase. We show that, for a fixed value of μ , the decrease of the size leads to a change in the order of the transition.

Possible extensions of this work are the investigation of properties of fermion-fermion condensates under finite-size conditions, as well as, the study of the system under the influence of an external magnetic field.

Acknowledgments

This work received partial financial support from CNPq and FAPERJ, Brazilian Agencies.

References

- [1] Y. Nambu, G. Jona-Lasinio, Phys. Rev. 122 (1961) 345; 124 (1961) 246.
- [2] S. P. Klevansky, Rev. Mod. Phys. 27 (1991) 195.
- [3] T. Hatsuda, T. Kunihiro, Phys. Rep. 247 (1994) 221.
- [4] M. Buballa, Phys. Rep. 407 (2005) 205.
- [5] D. K. Kim, Y. D. Han, I. G. Koh, Phys. Rev D 49 (1994) 6943.
- [6] Y. B. He, W. Q. Chao, C. S. Gao and X. Q. Li, Phys. Rev. C 54 (1996) 857.
- [7] J. B. Kogut, C. G. Strouthos, Phys.Rev. D 63 (2001) 054502.
- [8] C. G. Beneventano, E. M. Santangelo, J. Phys. A 37 (2004) 9261.

- [9] A. V. Gamayun, E. V. Gorbar, Phys. Lett. B 610 (2005) 74.
- [10] O. Kiriyaama, T. Kodama, T. Koide, e-Print: arXiv:hep-ph/0602086 (2006), and references therein.
- [11] L. M. Abreu, M. Gomes, A. J. da Silva, Phys. Lett. B 642 (2006) 551.
- [12] D. Ebert, K. G. Klimenko, A. V. Tyukov, V. C. Zhukovsky, Phys. Rev. D 78 (2008) 045008.
- [13] J. Braun, B. Klein, H.-J. Pirner, Phys.Rev. D 71 (2005) 014032.
- [14] J. Braun, B. Klein, H.-J. Pirner, A.H. Rezaeian, Phys.Rev. D 73 (2006) 074010.
- [15] E. Elizalde, *Ten physical applications of spectral zeta function*, Lecture Notes in Physics, Springer-Verlag, Berlin (1995).
- [16] O. Kiriyaama, A. Hosaka, Phys.Rev. D 67 (2003) 085010.
- [17] T. Inagaki, T. Kouno, T.Muta, Int. J. Mod. Phys. A 10 (1995) 2241.
- [18] B. R. Zhou, Commun. Theor. Phys. 39 (2003) 663.
- [19] K. Kirsten, J. Math. Phys. 35 (1994) 459.
- [20] L. M. Abreu, C. de Calan, A. P. C. Malbouisson, J. M. C. Malbouisson, A. E. Santana, J. Math. Phys. 46 (2005) 012304.
- [21] M. K. Volkov and A. E. Radzhabov, e-Print: arXiv:hep-ph/0508263 (2005).